Intrapleural Administration of AAV9 Improves Neural and Cardiorespiratory Function in Pompe Disease

Darin J Falk[1], Cathryn S Mah[1], Meghan S Soustek[1], Kun-Ze Lee[2], Mai K ElMallah[1], Denise A Cloutier[1], David D Fuller[2] and Barry J Byrne[1]

[1]Department of Pediatrics, College of Medicine, University of Florida, Gainesville, Florida, USA; [2]Department of Physical Therapy, College of Public Health and Health Professions, University of Florida, Gainesville, Florida, USA

Pompe disease is a neuromuscular disease resulting from deficiency in acid α-glucosidase (GAA), results in cardiac, skeletal muscle, and central nervous system (CNS) pathology. Enzyme replacement therapy (ERT) has been shown to partially correct cardiac and skeletal muscle dysfunction. However, ERT does not cross the blood–brain barrier and progressive CNS pathology ensues. We tested the hypothesis that intrapleural administration of recombinant adeno-associated virus (rAAV9)-GAA driven by a cytomegalovirus (CMV) or desmin (DES) promoter would improve cardiac and respiratory function in *Gaa*$^{-/-}$ mice through a direct effect and retrograde transport to motoneurons. Cardiac magnetic resonance imaging revealed significant improvement in ejection fraction in rAAV9-GAA–treated animals. Inspiratory phrenic and diaphragm activity was examined at baseline and during hypercapnic respiratory challenge. Mice treated with AAV9 had greater relative inspiratory burst amplitude during baseline conditions when compared with *Gaa*$^{-/-}$. In addition, efferent phrenic burst amplitude was significantly correlated with diaphragm activity in both AAV9-DES and AAV9-CMV groups but not in *Gaa*$^{-/-}$. This is the first study to indicate improvements in cardiac, skeletal muscle, and respiratory neural output following rAAV administration in Pompe disease. These results further implicate a role for the CNS in Pompe disease pathology and the critical need to target the neurologic aspects in developing therapeutic strategies.

Received 26 October 2012; accepted 4 April 2013; advance online publication 4 June 2013. doi:10.1038/mt.2013.96

INTRODUCTION

Pompe disease is a neuromuscular disease that leads to a severe and rapid development of cardiopulmonary and skeletal muscle dysfunction. The prevalence of Pompe (glycogen storage disease type II, acid maltase deficiency; MIM 232300) disease is ~1:40,000 live births worldwide and results from a single gene defect in acid α-glucosidase (GAA). Since GAA represents the only pathway for degradation of glycogen, once it reaches the lysosome there is significant glycogen accumulation. Pompe disease patients are affected by profound cardiac and skeletal muscle weakness and without intervention may die within 1 to 2 years. Although there is an Food and Drug Administration-approved therapy (enzyme replacement therapy (ERT)) for patients, this strategy only attenuates the skeletal muscle weakness associated with the disease. Even with ERT, patients nonetheless develop respiratory insufficiency and some require mechanical ventilation.[1,2] The lack of central nervous system (CNS) correction by ERT may be a primary mechanism for the failure to maintain sufficient alveolar ventilation. The overall success of ERT in Pompe patients has been in overall survival; however, 25% of early-onset patients die within the first 5 years of treatment and 65% of patients experience ventilatory insufficiency (reviewed in refs. 3–6). Successful treatment by ERT requires receptor-mediated uptake of GAA which is inefficient with currently available ERT formulations.[7] Treatment does however attenuate the progression of the disease,[2] with a high burden which requires life-long biweekly treatment and significant financial consequences (*i.e.,* average-size adult: ~$700,000/year). Therefore, our research focus is to develop a treatment option that more effectively addresses the pathophysiology of Pompe disease and may lead to improvements in the overall quality and duration of life in affected individuals.

Numerous clinical variants of Pompe disease have been observed and classified in patients. A continuum of disease is generally recognized, however, broad categories of severe/early-onset or mild/late-onset disease are traditionally used.[8] The disease severity is inversely correlated with residual GAA activity. The most severe form of the disease is due to complete absence of the enzyme and patients present in the first 3 months of life with congestive heart failure and severe hypotonia. There is progressive cardiomegaly and respiratory compromise that leads to cardiorespiratory failure in untreated patients within the first year of life. Later-onset forms of Pompe disease generally

Correspondence: *Barry J Byrne, University of Florida, Powell Gene Therapy Center, RG-148, 1200 Newell Drive, Gainesville, Florida 32610-0296, USA. E-mail: bbyrne@ufl.edu*

show 15–20% of normal GAA activity and predominantly have abnormalities in skeletal muscle (ambulatory and respiratory insufficiency); yet, cardiomyopathy and conduction abnormalities have been reported in adult patients (reviewed in ref. 8). Until recently, only cardiac and skeletal muscle involvement was acknowledged; however, additional studies have revealed glycogen accumulation in the brain and CNS.[2,9] Although lifespan has increased in patients receiving ERT, there is significant residual deficit in patients. Improved patients survival lead to a new management paradigm where patients face significant new challenges, especially related to ventilatory failure.[1,10] Therefore, our focus is to develop therapeutics options which will reverse and/or restore cardiac, neural, and skeletal muscle pathophysiology in affected patients.

A few reports have shown excessive glycogen deposition within the brain and CNS in Pompe patients[9,11–14] and *Gaa*$^{-/-}$ mice.[9,15,16] In the *Gaa*$^{-/-}$ model, studies have conclusively demonstrated pathology in respiratory motoneurons, including both the phrenic (diaphragm) and hypoglossal (tongue) motor pools. Neurophysiological recordings in adult *Gaa*$^{-/-}$ mice are consistent in showing a blunted efferent respiratory motor output as well as increased variability in the overall respiratory pattern.[9,17–19] In addition, direct C3-4 intraspinal injections with adeno-associated virus (AAV)-GAA restores spinal GAA and increased minute ventilation in *Gaa*$^{-/-}$ mice.[20] Importantly, respiratory parameters were attributed to a CNS-specific correction, since vector was delivered only to the spinal cord and no vector was detectable in the diaphragm of recombinant AAV (rAAV)-treated *Gaa*$^{-/-}$ animals. Therefore, accumulating evidence suggests that pathology in respiratory motoneurons and/or neural circuits is a major contribution to respiratory control problems in Pompe disease.

The rationale for intrapleural administration of rAAV vector was to address the primary disease manifestations in early-onset (cardiac and respiratory dysfunction) and late-onset (respiratory) Pompe patients. More importantly, intrapleural administration of vector may also provide sufficient retrograde transduction of phrenic and intercostal motor neurons,[21] thereby reversing respiratory dysfunction. We performed a direct comparison of a ubiquitous viral promoter (cytomegalovirus (CMV)) against a tissue-restricted promoter (desmin (DES)). The DES promoter contains a myocyte-specific enhancer factor 2 and a MyoD enhancer element and results in significant expression in the myocardium, diaphragm, and

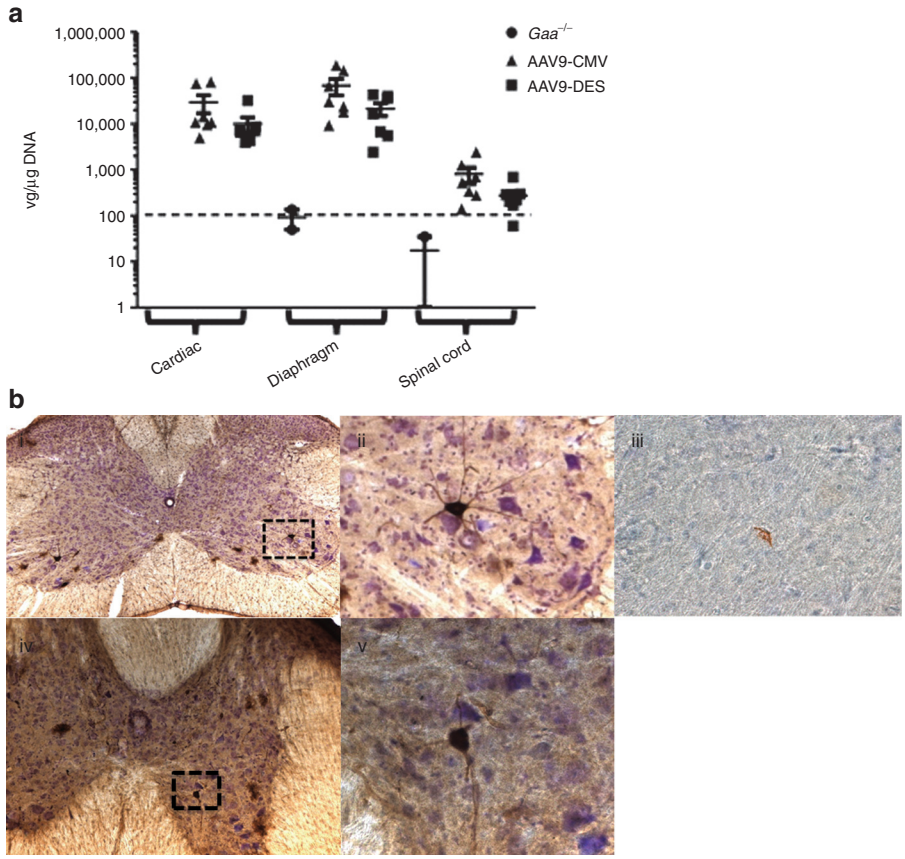

Figure 1 Vector genome quantification and retrograde transport of rAAV9 following intrapleural injection. (**a**) Vector copy number was significantly higher in cardiac, diaphragm, and the spinal cord in rAAV9-CMV or -DES *Gaa*$^{-/-}$ mice ($P < 0.05$). Data are presented as mean ± SEM. *Gaa*$^{-/-}$ = sham-treated *Gaa*$^{-/-}$, AAV9-CMV = rAAV9-CMV-hGAA + *Gaa*$^{-/-}$, AAV9-DES = rAAV9-DES-hGAA + *Gaa*$^{-/-}$. Dotted line represents threshold of detection. (**b**) Immunohistochemical detection of GFP staining in (i.) cervical and (iv.) thoracic spinal cord. Inset represents positive motoneuron (ii.) GFP, and (iii.) GAA staining in the cervical spinal cord and (v.) GFP staining in the thoracic spinal cord. CMV, cytomegalovirus; DES, desmin; GAA, acid α-glucosidase; GFP, green fluorescent protein; rAAV, recombinant adeno-associated virus; vg, vector genome.

CNS.[22] The present study explores the feasibility of intrapleural administration for transduction of the myocardium, respiratory muscles, and CNS for treatment of Pompe disease.

RESULTS

To compare the therapeutic efficacy of rAAV9-mediated gene delivery, 3 months old *Gaa*$^{-/-}$ mice were treated with a single intrapleural injection of rAAV9-CMV-hGAA (AAV9-CMV) or rAAV9-DES-hGAA (AAV9-DES) (1×10^{11} vector genome/mouse). Cardiac, neurophysiologic, and respiratory indexes were assessed 6 months post-injection.

Viral genome distribution of rAAV9 following intrapleural delivery

The transduction efficiency of rAAV9-hGAA in the spinal cord, myocardium, and diaphragm was assessed by real-time PCR. Six months following vector administration, real-time PCR analysis showed detection of vector genome copies in the cervical/thoracic spinal cord, diaphragm, and myocardium (**Figure 1**). Immunohistochemical examination of the cervical and thoracic spinal cord regions following intrapleural injection of rAAV9-green fluorescent protein (GFP) was performed in *Gaa*$^{-/-}$ mice. Positive immunolabeling for GFP was observed in the phrenic and costal motoneuron pool (**Figure 1b**, **i**, **ii**, **iv**, **v**). Positive immunolabeling of GAA in the phrenic motoneuron pool was observed in AAV9-DES-GAA–treated animals at 6 months post-injection (**Figure 1b**, **iii**). Transgene expression in motoneurons and detection of viral genomes in spinal cord suggest retrograde transport of rAAV9 vector[19] following intrapleural delivery.

Intrapleural delivery of rAAV9 results in significant GAA activity and glycogen clearance in cardiac and respiratory muscles

Previously, we have shown that rAAV gene transfer to the myocardium and respiratory muscles results in a significant increase in GAA activity. In this study at 6 months post-injection, cardiac GAA activity levels were 23.0 ± 8.9 and 61.8 ± 29.8% of wild-type in AAV9-CMV– and AAV9-DES–treated animals ($P < 0.05$), respectively (**Figure 2a**). Elevation of GAA activity was also observed in the diaphragm (**Figure 2b**, AAV9-CMV 115.8 ± 27.9%; AAV9-DES 40.3 ± 9.8%; $P < 0.05$) and costal muscles (data not shown) of AAV9 vector-treated animals. No increase in liver GAA activity levels was detected in AAV9 vector-treated animals (**Figure 2c**). Staining for glycogen by periodic acid-Schiff's staining revealed a reduction in lysosomal glycogen deposition in AAV9-treated animals in the diaphragm (**Figure 2d**), myocardium, and costal muscles (data not shown).

Cardiac function

Early-onset Pompe patients and *Gaa*$^{-/-}$ mice demonstrate profound cardiac hypertrophy and dysfunction.[1] Intravenous administration of rAAV1-GAA has been shown to improve cardiac function and reduce left ventricular mass in *Gaa*$^{-/-}$ mice.[23]

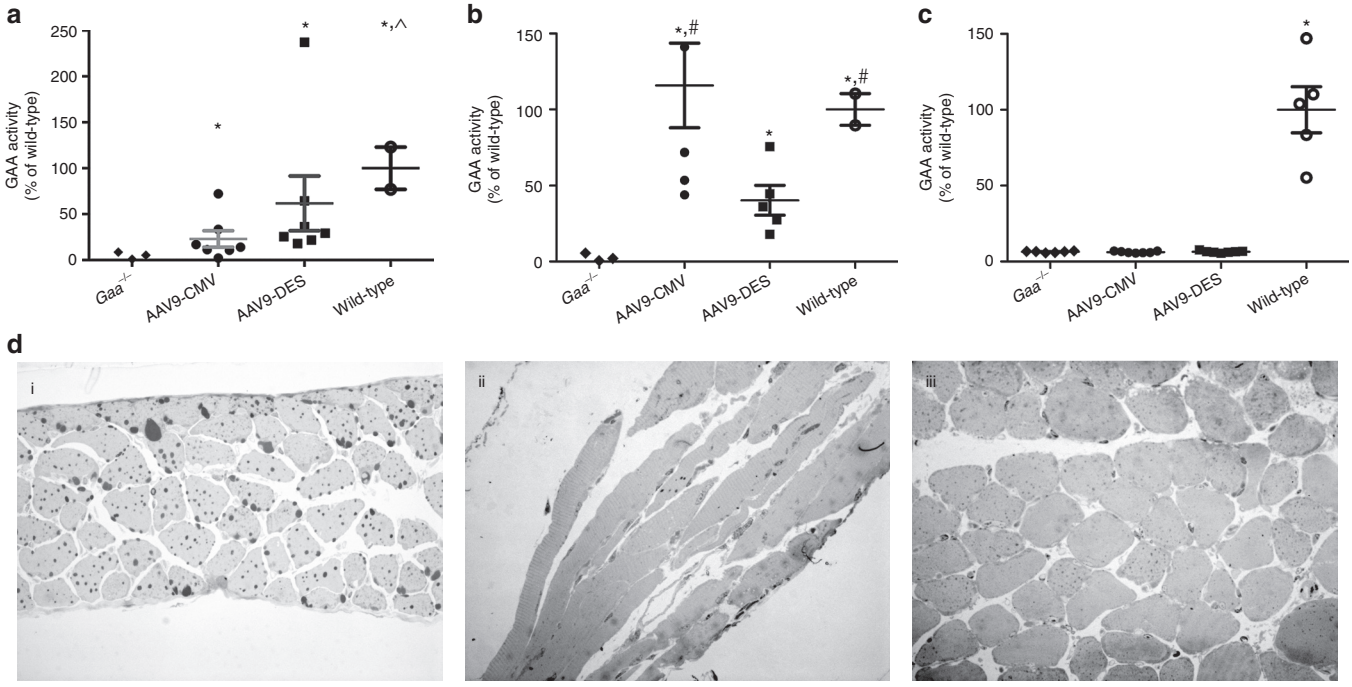

Figure 2 GAA activity and glycogen detection following intrapleural injection. GAA activity in the (**a**) myocardium, (**b**) diaphragm, and (**c**) liver 6 months after rAAV9 vector delivery in *Gaa*$^{-/-}$ mice ($P < 0.05$). (**d**) Representative sections of (i.) *Gaa*$^{-/-}$, (ii.) AAV9-CMV, and (iii.) AAV9-DES stained for glycogen in the diaphragm using PAS staining. Although glycogen (intense black staining) is still visible in AAV9 vector-treated animals, it appears there is a severe reduction in the overall number and size of deposition. Data are presented as mean ± SEM. *Gaa*$^{-/-}$ = sham-treated *Gaa*$^{-/-}$, AAV9-CMV = rAAV9-CMV-hGAA + *Gaa*$^{-/-}$, AAV9-DES = rAAV9-DES-hGAA + *Gaa*$^{-/-}$, WT = wild-type (129SVE). *$P < 0.05$ compared with untreated *Gaa*$^{-/-}$; ^$P < 0.05$ compared with AAV9-CMV; $^{\#}P < 0.05$ compared with AAV9-DES. CMV, cytomegalovirus; DES, desmin; GAA, acid α-glucosidase; PAS, periodic acid-Schiff; rAAV, recombinant adeno-associated virus.

High-field (4.7-T) cardiac magnetic resonance imaging done 6 months post-dose revealed significant improvement in ejection fraction (AAV9-DES: 74.9 ± 4.9 and AAV9-CMV: 74.1 ± 4.5, $P < 0.05$) and stroke volume (AAV9-DES: 41.2 ± 2.6 and AAV9-CMV: 38.2 ± 3.1, $P < 0.05$) when compared with *Gaa*$^{-/-}$ animals (66.7 ± 1.8 and 30.5 ± 1.0, ejection fraction and stroke volume, respectively) (**Figure 3a**,**b**).

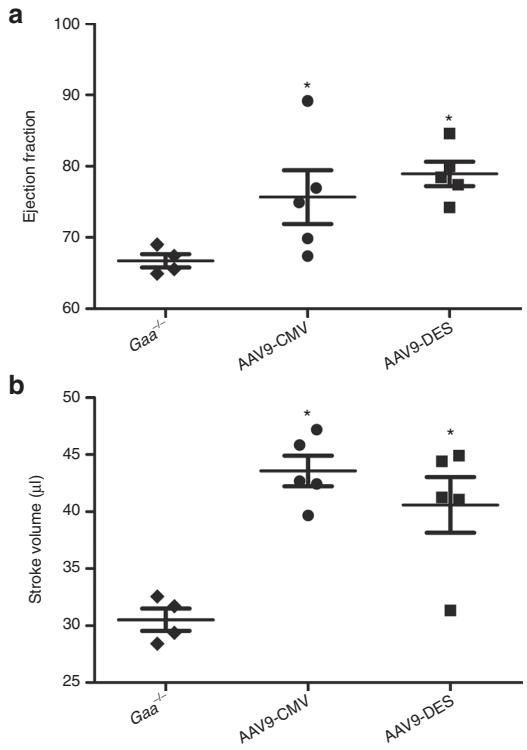

Figure 3 Assessment of cardiac function at 4.7-T. (**a**) Cardiac magnetic resonance imaging detected improved ejection fraction and (**b**) stroke volume in rAAV9-treated *Gaa*$^{-/-}$ mice ($P < 0.05$). *Gaa*$^{-/-}$ = sham-treated *Gaa*$^{-/-}$, AAV9-CMV = rAAV9-CMV-hGAA + *Gaa*$^{-/-}$, AAV9-DES = rAAV9-DES-hGAA + *Gaa*$^{-/-}$. *$P < 0.05$ compared with untreated *Gaa*$^{-/-}$. CMV, cytomegalovirus; DES, desmin; GAA, acid α-glucosidase; rAAV, recombinant adeno-associated virus.

Impact of rAAV-hGAA on respiratory function in *Gaa*$^{-/-}$ mice

Respiratory-related electrical discharges were recorded from both the phrenic nerve (neurograms) and the diaphragm (electromyograms (EMG)) in spontaneously breathing, anesthetized mice. We detected no impact of AAV9-GAA treatment on the inspiratory frequency (breaths × min^{-1}; **Figure 4a**). However, assessment of inspiratory bursting suggested increased respiratory motor drive in *Gaa*$^{-/-}$ mice following AAV9-GAA treatment. **Figure 4b** depicts the amplitude of the inspiratory phrenic burst expressed relative to peak activity evoked by a brief hypercapnic stimulus. *Gaa*$^{-/-}$ mice treated with AAV9-DES and AAV9-CMV both showed a significantly greater inspiratory phrenic burst, possibly indicating greater or more efficient phrenic motoneuron recruitment compared with the baseline ventilation conditions. In contrast, we did not detect a significant impact of either AAV9-GAA vector on the burst amplitude of the normalized diaphragm EMG signal (**Figure 4c**). This may reflect the inability of the EMG electrodes to effectively sample all active diaphragm motor units given the technical limitations of the diaphragm EMG in mice. It is of potential interest, however, to note that there was a strong tendency for the raw amplitude (*i.e.*, arbitrary units) of the diaphragm EMG signal to be enhanced in mice treated with the AAV9-DES vector (data not shown). Simultaneously recording the electrical activity of the phrenic nerve and diaphragm enabled us to examine the relationship between these two variables. We found no detectable correlation between phrenic nerve output and diaphragm activity in untreated *Gaa*$^{-/-}$ mice ($r^2 = 0.00$), suggesting a problem with neuromuscular transmission in *Gaa*$^{-/-}$ mice. In contrast to the untreated group, *Gaa*$^{-/-}$ mice treated with both AAV9-CMV ($r^2 = 0.67$, $P < 0.05$) and AAV9-DES ($r^2 = 0.60$, $P < 0.05$) showed a significant relationship between phrenic nerve activity and diaphragm EMG output (**Figure 5**). Accordingly, AAV9 treatment may have acted to restore or enhance neuromuscular transmission between the phrenic nerve and the diaphragm.

DISCUSSION

The current study addresses several key issues specific to Pompe disease. First, it is generally accepted that ERT increases lifespan in Pompe patients but fails to result in a substantial increase in

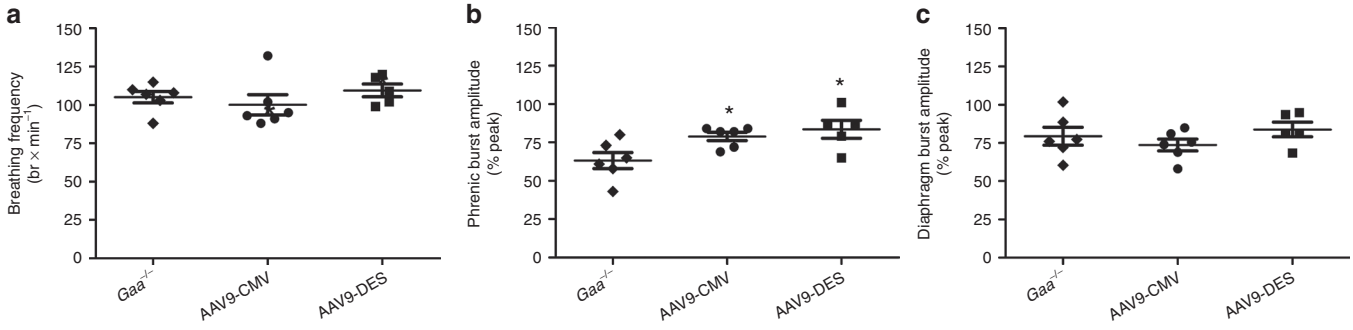

Figure 4 The impact of AAV-GAA therapy on respiratory motor output in anesthetized Gaa$^{-/-}$ mice. (**a**) Breathing frequency was similar between control, untreated *Gaa*$^{-/-}$ mice and those injected with AAV. (**b**) However, the normalized amplitude of the efferent phrenic inspiratory burst was significantly greater in both AAV9-CMV– and AAV9-DES–treated mice. (**c**) The efferent diaphragm burst was also normalized to peak output, but this analysis revealed no differences between the groups. *Gaa*$^{-/-}$ = sham-treated *Gaa*$^{-/-}$, AAV9-CMV = rAAV9-CMV-hGAA + *Gaa*$^{-/-}$, AAV9-DES = rAAV9-DES-hGAA + *Gaa*$^{-/-}$, WT = wild-type (129SVE). *$P < 0.05$ compared with untreated *Gaa*$^{-/-}$. CMV, cytomegalovirus; DES, desmin; GAA, acid α-glucosidase; rAAV, recombinant adeno-associated virus.

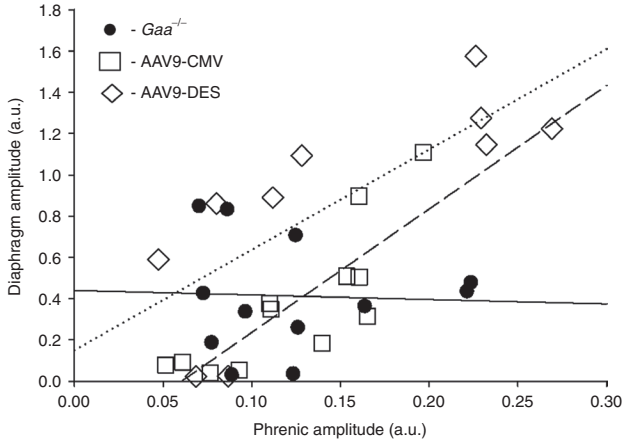

Figure 5 The relationship between efferent phrenic burst amplitude and diaphragm burst amplitude. Anesthetized mice were studied during spontaneous breathing, and the raw burst amplitudes (*i.e.,* arbitrary units (a.u.)) of the inspiratory phrenic neurograms and diaphragm EMG were analyzed. Untreated *Gaa*$^{-/-}$ mice showed no relationship between these variables, but both groups of AAV9-treated mice had a linear relationship. The lines indicate the linear regression as follows: solid line: *Gaa*$^{-/-}$; dotted line: AAV9-DES; dashed line: AAV9-CMV. AAV, adeno-associated virus; CMV, cytomegalovirus; DES, desmin; EMG, electromyogram; GAA, acid α-glucosidase.

lysosomal GAA levels, decreased glycogen content, and improved respiratory function. Primarily, these events are believed to occur as a result of inefficient cation-independent mannose 6-phospate receptor-mediated uptake. The direct correction of affected cells *via* rAAV-mediated GAA delivery has been shown to increase cellular GAA levels through a cell autonomous mechanism utilizing the high efficiency of the intracellular trafficking pathway. A lack of detectable GAA enzymatic activity in liver lysates from AAV9-treated animals following intrapleural administration supports a cell autonomous mechanism. Our results show this mechanism results in a significant increase in lysosomal GAA activity and leads to a depletion of lysosomal glycogen and improved cardiac and respiratory function. Second, many reports investigating alternative therapies have focused on skeletal muscle morphology or integrated neuromuscular measurements (*i.e.,* wire hang, rotorod) to determine efficacy. We have extended upon previous observations and incorporated *in vivo* neurophysiologic and EMG analyses to delineate the tissue-specific effects of rAAV-mediated gene transfer. Lastly, the effect of rAAV treatment in regard to cardiac morphology and function has been included in this report as it is the principal manifestation in infantile Pompe patients. Overall, our results suggest that rAAV therapy can mitigate the cardiac, motoneuron, and respiratory complications associated with Pompe disease.

Numerous reports have shown a significant increase in cardiac GAA activity,[1] and improved cardiac function and morphology[23–25] following rAAV-hGAA delivery in the *Gaa*$^{-/-}$ mouse model. However, an augmentation of ejection fraction and decrease in left ventricular mass has only been reported following intravenous delivery of rAAV1 vectors.[26] Here, we show long-term improvement (6 months) in ejection fraction and stroke volume in rAAV9-treated animals. Due to the severe cardiomegaly in early-onset patients,[27] effective therapy should address efficient myocardial transduction and glycogen clearance to normalize cardiac function.

Direct intramuscular, hepatic, limb perfusion, or intravenous delivery of rAAV have resulted in increased GAA activity in skeletal muscle. Importantly, vector-mediated GAA production appears to be fiber-type–independent in contrast to a preferential type I fiber phenotype receptor-mediated and trafficking to the lysosome by ERT.[28] Moreover, intravenous delivery of rAAV-GAA vectors has resulted in a significant increase in skeletal muscle-specific force production in predominantly type I fibers of the soleus[26,29] and a mixed fiber phenotype muscle like the diaphragm.[17,23,30] Respiratory insufficiency is the primary contributor to late-onset disease. Mechanical ventilation in itself contributes diaphragmatic contractile dysfunction and atrophy;[31] this coupled with excessive myofiber glycogen accumulation is likely to worsen ventilator-induced diaphragm dysfunction.

Perhaps most significant is the increasing prevalence of reports describing CNS pathology in Pompe disease.[9,11–16,18,32,33] Previously, we have shown reduced ventilatory function in a muscle-specific GAA transgenic mouse model, whereas *ex vivo* diaphragmatic contractile function is corrected by the expression of GAA. These findings have major implications, since *ex vivo* diaphragmatic contractile function is assessed independent from neural input. As numerous factors could contribute to respiratory deficits independent of GAA expression in a muscle-specific model, the ventilatory dysfunction is likely the result of motoneuron dysfunction. This was confirmed through several recent reports demonstrating impaired hypoglossal and phrenic motor output in *Gaa*$^{-/-}$ mice.[9,17,18] However, there is only one report describing direct clearance of motoneuron glycogen deposition and improved respiratory function in *Gaa*$^{-/-}$ following rAAV therapy.[20] The study by Qui *et al.* demonstrated high transduction of the ventral cervical spinal cord, including the phrenic motoneuron pool, and significant improvements in minute ventilation following direct spinal rAAV delivery. The increase in ventilation after direct spinal AAV-GAA delivery highlights a role for neuropathology as a significant mechanism of respiratory insufficiency in Pompe disease. Accumulation of glycogen could lead to motoneuron and interneuron dysfunction and death.[34] Since ERT does not cross the blood–brain barrier, ERT has no effect on CNS glycogen deposition. Therefore, the effect of direct transduction of motor neurons by vector-mediated delivery is expected to lead to a greater degree of respiratory correction in Pompe disease.[9]

The severity of cardiac disease in the Pompe patient population is dependent on the residual enzyme activity and degree of glycogen accumulation. In this study, we evaluated the intrapleural route of administration to efficiently target the myocardium, respiratory muscles, and neurons. Although systemic administration would result in increased biodistribution, intrapleural delivery may provide an avenue to target key respiratory muscles and the myocardium with a higher amount of vector genomes. Previously, intrapleural delivery of rAAV vectors has been shown to transduce the diaphragm, costal muscles, myocardium, and lung.[35,36] The impact on cardiopulmonary function following intrapleural vector delivery has not been previously investigated. In this study, modulation of GAA through intrapleural delivery of rAAV augments cardiac and respiratory function in adult *Gaa*$^{-/-}$ mice.

Vector administration occurred at 3 months of age when tissues from *Gaa*$^{-/-}$ mice already display pathology; however, long-term expression and physiological correction was observed 6 months post-injection. Importantly, the improvement in respiratory function was the result of gene transfer to respiratory muscles and motoneurons. Transduction of phrenic and costal motoneurons is in agreement with previous work demonstrating the retrograde transport ability and/or blood–brain barrier permissibility of rAAV9 vectors.[19,37,38] The current mechanism by which rAAV9 is retrogradely transported following direct intramuscular injection has not been defined. It is conceivable that viral uptake occurs at the neuromuscular junction but to our knowledge this has not been definitively evaluated. Axonal transport of rAAV appears to be serotype-dependent and is enhanced when N-methyl D-aspartate receptor antagonist (histogranin) and dynein-related peptide sequences are inserted into VP3.[39–42] Elucidating the mechanism by which rAAV is transported between skeletal muscle and peripheral nerves may enable the alteration of capsid composition to enhance or diminish retrograde transport ability, thereby improving therapy. Overall our findings support the causative role of the CNS for the development of respiratory muscle weakness and warrant continued development of rAAV-based therapies for the treatment of inherited myopathies and neuromuscular disease.

MATERIALS AND METHODS

Packaging and purification of rAAV9 vectors. Recombinant AAV9 vectors were produced using the triple plasmid transfection method, purified, and titered as previously described.[43] The AAV9 packaging plasmid pRep2/Cap9 was a kind gift from Dr James Wilson (University of Pennsylvania, Philadelphia, PA).

Experimental animals. The *Gaa*$^{-/-}$ mouse (Taconic, Hudson, NY) originally developed by Raben *et al.*[44] was outbred to a 129SVE background. Three months old *Gaa*$^{-/-}$ male and female mice were randomized to the following groups: untreated *Gaa*$^{-/-}$ + lactated ringer's solution or AAV9-GFP (CON), *Gaa*$^{-/-}$ + AAV9-DES-hGAA (DES), *Gaa*$^{-/-}$ + AAV9-CMV-hGAA (CMV), and compared with the syngeneic background strain 129SVE + lactated ringer's solution (wild-type). All animal studies were approved in accordance with the guidelines set forth by the University of Florida Institutional Animal Care and Use Committee. All animals were sacrificed at 9 months of age (6 months post-injection) for molecular, histologic, and biochemical assays.

In vivo *delivery of rAAV vector.* Mice were anesthetized using 2% isoflurane (1l O_2). Under sterile conditions, mice were injected with a single injection using an insulin tuberculin syringe. Lactated ringers solution or rAAV9 (1×10^{11} vector genome) diluted with lactated ringers solution to a quantity sufficient volume of 400 µl was used for intrapleural delivery.

Cardiac measurements. Cardiac magnetic resonance imaging was performed on a 4.7-T Bruker Avance spectrometer (Bruker BioSpin, Billerica, MA) at the University of Florida AMRIS facility. The animals were anesthetized using 1.5% isoflurane and 1 l/minute oxygen. The animals were placed prone on a home-built quadrature transmit-and-receive surface coil, with the heart placed at the center of the coil. Images were acquired using IntraGate and were retrospectively reconstructed. The heart was visualized by acquiring single short-axis slices along the length of the left ventricle. Images were processed using CAAS MRV for mouse (Pie Medical Imaging, Maastricht, The Netherlands). Contours were drawn for the epicardium and the endocardium for each slice along the length of the left ventricle at both end diastole and end systole. The results were exported and analyzed and ejection fraction% and stroke volume was calculated.

Recording phrenic nerve and diaphragm electrical activity during spontaneous breathing. All procedures were adapted from our prior reports.[9,18] Mice were anesthetized with urethane (1.0–1.6 g/kg, intraperitoneally; Sigma, St Louis, MO) and studied while in a supine position. A servo-controlled heating pad enabled regulation of body temperature at 37–38 °C (model TC-1000; CWE, Ardmore, PA). Mice were spontaneously breathing throughout these experiments. Inspired oxygen was maintained at 50% (balance N_2), and monitored *via* O_2 sensor (Model GB300; Teledyne Technologies, City of Industry, CA). The phrenic nerve was isolated unilaterally and nerve activity was recorded using a monopolar silver wire electrode (no. 782500; A-M Systems, Carlsborg, WA). The signal was amplified (1000x, Model 1700; A-M Systems, Carlsborg, WA) and band-pass filtering (0.3–10 kHz). The raw neurograms were integrated using a 100-ms time constant (model MA-1000; CWE). In addition to phrenic nerve activity, electrical activity was simultaneously recorded from the abdominal surface of the diaphragm using a bipolar surface electrode consisting of two stainless steel wires. The signal was amplified (1000x) and filtered (band pass: 0.3–10 kHz; notch: 60 Hz) using a differential A/C amplifier (Model 1700; A-M Systems). The signal was also rectified and moving averaged (time constant: 100 ms, MA-1000 moving averager; CWE). All signals were digitized and recorded on a PC using Spike2 software (Cambridge Electronic Design Limited, Cambridge, England).

Biochemical Assessment. At 6 months post-injection, tissue homogenates were assayed for GAA enzyme activity as described previously.[29] Briefly, tissue lysates were assayed for GAA activity by measuring the cleavage of 4-methylumbelliferyl-α-D-glucoside (Sigma M9766; Sigma) after 1-hour incubation at 37 °C.

Histological analysis. Cardiac and diaphragm samples were fixed immediately in 3% glutaldehyde in 0.2 mol/l Na Cacodylate buffer (pH 7.3) before embedding in epon as described previously[45] with minor modifications. Briefly, tissues were incubated in 0.5% periodic acid (Richard-Allan Scientific, Kalamazoo, MI) for 10 minutes at 60 °C, rinsed with tap water and then stained with Schiff's reagent (Richard-Allan Scientific) for 5 minutes, and then rinsed again in tap water. Sections were then counterstained with toluidine blue for 10–20 seconds. GFP immunohistochemistry of the cervical and thoracic spinal cord following rAAV9-GFP was performed according to ElMallah *et al.*[19] Briefly, GFP immunohistochemistry was performed by secondary detection with a VECTASTAIN ABC kit (Vector Laboratories, Burlingame, CA) and DAB. Tissue was incubated overnight with primary antibody against GFP, diluted 1:20,000 (chicken anti-GFP; Aves Laboratories, Tigard, OR). Sections were washed in phosphate-buffered saline, incubated with a biotinylated anti-chicken IgG secondary antibody (diluted 1:200; Vector Laboratories), and treated with a VECTASTAIN ABC kit and DAB for detection *via* bright-field microscopy.

Vector pharmacology. Real-time DNA PCR detection was performed as previously described.[17] Tissues samples from animals in each group were analyzed and data are reported as AAV vector genome copies per µg DNA ± SEM.

Statistical analyses. Statistical studies were performed using GraphPad Prism or SigmaStat v2.0 software (Graphpad Software, La Jolla, CA). The peak height of the inspiratory signals recorded in the phrenic nerve and diaphragm during the baseline condition was normalized to the value during hypercapnic challenge (% peak). Both amplitude of respiratory motor output and respiratory frequency were analyzed by one-way analysis of variance followed by Student–Newman–Keuls post-hoc test. A linear regression analysis was used to evaluate relationship between the non-normalized burst amplitude (*i.e.,* arbitrary units) recorded in the phrenic nerve and the diaphragm. Descriptive statistics were used for each group, and one-way analysis of variance, followed by Tukey's post-hoc comparison if necessary was used among groups. All results are presented as mean ± SE. $P < 0.05$ was considered significant.

ACKNOWLEDGMENTS

The authors gratefully acknowledge the University of Florida Powell Gene Therapy Center Vector Core Laboratory for production and titering of recombinant adeno-associated virus vectors and the University of Florida Toxicology Core (Thomas Conlon and Kirsten Erger) for vector genome analysis. This work was supported by grants from the National Institutes of Health (NHLBI-F32HL095282 and MDA 216676 (D.J.F.), NHLBI PO1 HL59412-06 (B.J.B.), 1R01HD052682-01A1 (D.D.F.), 15T32HL083810-04 (M.S.S.), Parker B. Francis (M.K.E.)). The content is solely the responsibility of the authors and does not necessarily represent the official views of the National Heart, Lung, and Blood Institute or the National Institutes of Health. B.J.B., D.D.F., The Johns Hopkins University, and the University of Florida could be entitled to patent royalties for inventions described in this manuscript. The authors declared no conflict of interest.

REFERENCES

1. Byrne, BJ, Falk, DJ, Pacak, CA, Nayak, S, Herzog, RW, Elder, ME *et al.* (2011). Pompe disease gene therapy. *Hum Mol Genet* **20**(R1): R61–R68.
2. Byrne, BJ, Kishnani, PS, Case, LE, Merlini, L, Müller-Felber, W, Prasad, S *et al.* (2011). Pompe disease: design, methodology, and early findings from the Pompe Registry. *Mol Genet Metab* **103**: 1–11.
3. Burrow, TA, Hopkin, RJ, Leslie, ND, Tinkle, BT and Grabowski, GA (2007). Enzyme reconstitution/replacement therapy for lysosomal storage diseases. *Curr Opin Pediatr* **19**: 628–635.
4. Fukuda, T, Roberts, A, Plotz, PH and Raben, N (2007). Acid alpha-glucosidase deficiency (Pompe disease). *Curr Neurol Neurosci Rep* **7**: 71–77.
5. Geel, TM, McLaughlin, PM, de Leij, LF, Ruiters, MH and Niezen-Koning, KE (2007). Pompe disease: current state of treatment modalities and animal models. *Mol Genet Metab* **92**: 299–307.
6. Raben, N, Plotz, P and Byrne, BJ (2002). Acid alpha-glucosidase deficiency (glycogenosis type II, Pompe disease). *Curr Mol Med* **2**: 145–166.
7. Coutinho, MF, Prata, MJ and Alves, S (2012). Mannose-6-phosphate pathway: a review on its role in lysosomal function and dysfunction. *Mol Genet Metab* **105**: 542–550.
8. Kishnani, PS, Steiner, RD, Bali, D, Berger, K, Byrne, BJ, Case, LE *et al.* (2006). Pompe disease diagnosis and management guideline. *Genet Med* **8**: 267–288.
9. DeRuisseau, LR, Fuller, DD, Qiu, K, DeRuisseau, KC, Donnelly, WH Jr, Mah, C *et al.* (2009). Neural deficits contribute to respiratory insufficiency in Pompe disease. *Proc Natl Acad Sci USA* **106**: 9419–9424.
10. Kishnani, PS, Corzo, D, Nicolino, M, Byrne, B, Mandel, H, Hwu, WL *et al.* (2007). Recombinant human acid [alpha]-glucosidase: major clinical benefits in infantile-onset Pompe disease. *Neurology* **68**: 99–109.
11. Mancall, EL, Aponte, GE and Berry, RG (1965). Pompe's disease (diffuse glycogenosis) with neuronal storage. *J Neuropathol Exp Neurol* **24**: 85–96.
12. Gambetti, P, DiMauro, S and Baker, L (1971). Nervous system in Pompe's disease. Ultrastructure and biochemistry. *J Neuropathol Exp Neurol* **30**: 412–430.
13. Martin, JJ, de Barsy, T, van Hoof, F and Palladini, G (1973). Pompe's disease: an inborn lysosomal disorder with storage of glycogen. A study of brain and striated muscle. *Acta Neuropathol* **23**: 229–244.
14. Teng, YT, Su, WJ, Hou, JW and Huang, SF (2004). Infantile-onset glycogen storage disease type II (Pompe disease): report of a case with genetic diagnosis and pathological findings. *Chang Gung Med J* **27**: 379–384.
15. Matsui, T, Kuroda, S, Mizutani, M, Kiuchi, Y, Suzuki, K and Ono, T (1983). Generalized glycogen storage disease in Japanese quail (Coturnix coturnix japonica). *Vet Pathol* **20**: 312–321.
16. Sidman, RL, Taksir, T, Fidler, J, Zhao, M, Dodge, JC, Passini, MA *et al.* (2008). Temporal neuropathologic and behavioral phenotype of 6neo/6neo Pompe disease mice. *J Neuropathol Exp Neurol* **67**: 803–818.
17. Mah, CS, Falk, DJ, Germain, SA, Kelley, JS, Lewis, MA, Cloutier, DA *et al.* (2010). Gel-mediated delivery of AAV1 vectors corrects ventilatory function in Pompe mice with established disease. *Mol Ther* **18**: 502–510.
18. Lee, KZ, Qiu, K, Sandhu, MS, Elmallah, MK, Falk, DJ, Lane, MA *et al.* (2011). Hypoglossal neuropathology and respiratory activity in pompe mice. *Front Physiol* **2**: 31.
19. ElMallah, MK, Falk, DJ, Lane, MA, Conlon, TJ, Lee, KZ, Shafi, NI *et al.* (2012). Retrograde gene delivery to hypoglossal motoneurons using adeno-associated virus serotype 9. *Hum Gene Ther Methods* **23**: 148–156.
20. Qiu, K, Falk, DJ, Reier, PJ, Byrne, BJ and Fuller, DD (2012). Spinal delivery of AAV vector restores enzyme activity and increases ventilation in Pompe mice. *Mol Ther* **20**: 21–27.
21. Mantilla, CB, Zhan, WZ and Sieck, GC (2009). Retrograde labeling of phrenic motoneurons by intrapleural injection. *J Neurosci Methods* **182**: 244–249.
22. Pacak, CA, Sakai, Y, Thattaliyath, BD, Mah, CS and Byrne, BJ (2008). Tissue specific promoters improve specificity of AAV9 mediated transgene expression following intravascular gene delivery in neonatal mice. *Genet Vaccines Ther* **6**: 13.
23. Mah, C, Pacak, CA, Cresawn, KO, Deruisseau, LR, Germain, S, Lewis, MA *et al.* (2007). Physiological correction of Pompe disease by systemic delivery of adeno-associated virus serotype 1 vectors. *Mol Ther* **15**: 501–507.
24. Pacak, CA, Mah, C, Cresawn, KO, Lewis, MA, Germain, S and Byrne, BJ (2006). rAAV2/9 mediated gene delivery of acid α-glucosidase corrects the cardiac phenotype in a mouse model of Pompe disease. American Society of Gene Therapy 9th Annual Meeting, **vol. 13**. Molecular Therapy: Baltimore, MD.
25. Mah, C, Cresawn, KO, Fraites, TJ Jr, Pacak, CA, Lewis, MA, Zolotukhin, I *et al.* (2005). Sustained correction of glycogen storage disease type II using adeno-associated virus serotype 1 vectors. *Gene Ther* **12**: 1405–1409.
26. Cresawn, KO, Fraites, TJ, Wasserfall, C, Atkinson, M, Lewis, M, Porvasnik, S *et al.* (2005). Impact of humoral immune response on distribution and efficacy of recombinant adeno-associated virus-derived acid alpha-glucosidase in a model of glycogen storage disease type II. *Hum Gene Ther* **16**: 68–80.
27. van den Hout, HM, Hop, W, van Diggelen, OP, Smeitink, JA, Smit, GP, Poll-The, BT *et al.* (2003). The natural course of infantile Pompe's disease: 20 original cases compared with 133 cases from the literature. *Pediatrics* **112**: 332–340.
28. Raben, N, Roberts, A and Plotz, PH (2007). Role of autophagy in the pathogenesis of Pompe disease. *Acta Myol* **26**: 45–48.
29. Fraites, TJ Jr, Schleissing, MR, Shanely, RA, Walter, GA, Cloutier, DA, Zolotukhin, I *et al.* (2002). Correction of the enzymatic and functional deficits in a model of Pompe disease using adeno-associated virus vectors. *Mol Ther* **5**(5 Pt 1): 571–578.
30. Rucker, M, Fraites, TJ Jr, Porvasnik, SL, Lewis, MA, Zolotukhin, I, Cloutier, DA *et al.* (2004). Rescue of enzyme deficiency in embryonic diaphragm in a mouse model of metabolic myopathy: Pompe disease. *Development* **131**: 3007–3019.
31. Powers, SK, Kavazis, AN and Levine, S (2009). Prolonged mechanical ventilation alters diaphragmatic structure and function. *Crit Care Med* **37** (suppl. 10): S347–S353.
32. Hogan, GR, Gutmann, L, Schmidt, R and Gilbert, E (1969). Pompe's disease. *Neurology* **19**: 894–900.
33. Burrow, TA, Bailey, LA, Kinnett, DG and Hopkin, RJ (2010). Acute progression of neuromuscular findings in infantile Pompe disease. *Pediatr Neurol* **42**: 455–458.
34. Bellettato, CM and Scarpa, M (2010). Pathophysiology of neuropathic lysosomal storage disorders. *J Inherit Metab Dis* **33**: 347–362.
35. Blankinship, MJ, Gregorevic, P, Allen, JM, Harper, SQ, Harper, H, Halbert, CL *et al.* (2004). Efficient transduction of skeletal muscle using vectors based on adeno-associated virus serotype 6. *Mol Ther* **10**: 671–678.
36. Tarantal, AF and Lee, CC (2010). Long-term luciferase expression monitored by bioluminescence imaging after adeno-associated virus-mediated fetal gene delivery in rhesus monkeys (Macaca mulatta). *Hum Gene Ther* **21**: 143–148.
37. Foust, KD, Nurre, E, Montgomery, CL, Hernandez, A, Chan, CM and Kaspar, BK (2009). Intravascular AAV9 preferentially targets neonatal neurons and adult astrocytes. *Nat Biotechnol* **27**: 59–65.
38. Zheng, H, Qiao, C, Wang, CH, Li, J, Li, J, Yuan, Z *et al.* (2010). Efficient retrograde transport of adeno-associated virus type 8 to spinal cord and dorsal root ganglion after vector delivery in muscle. *Hum Gene Ther* **21**: 87–97.
39. Salegio, EA, Samaranch, L, Kells, AP, Mittermeyer, G, San Sebastian, W, Zhou, S *et al.* (2013). Axonal transport of adeno-associated viral vectors is serotype-dependent. *Gene Ther* **20**: 348–352.
40. Kells, AP, Hadaczek, P, Yin, D, Bringas, J, Varenika, V, Forsayeth, J *et al.* (2009). Efficient gene therapy-based method for the delivery of therapeutics to primate cortex. *Proc Natl Acad Sci USA* **106**: 2407–2411.
41. Xu, J, Ma, C, Bass, C and Terwilliger, EF (2005). A combination of mutations enhances the neurotropism of AAV-2. *Virology* **341**: 203–214.
42. Schnapp, BJ and Reese, TS (1989). Dynein is the motor for retrograde axonal transport of organelles. *Proc Natl Acad Sci USA* **86**: 1548–1552.
43. Zolotukhin, S, Potter, M, Zolotukhin, I, Sakai, Y, Loiler, S, Fraites, TJ Jr *et al.* (2002). Production and purification of serotype 1, 2, and 5 recombinant adeno-associated viral vectors. *Methods* **28**: 158–167.
44. Raben, N, Nagaraju, K, Lee, E, Kessler, P, Byrne, B, Lee, L *et al.* (1998). Targeted disruption of the acid alpha-glucosidase gene in mice causes an illness with critical features of both infantile and adult human glycogen storage disease type II. *J Biol Chem* **273**: 19086–19092.
45. Lynch, CM, Johnson, J, Vaccaro, C and Thurberg, BL (2005). High-resolution light microscopy (HRLM) and digital analysis of Pompe disease pathology. *J Histochem Cytochem* **53**: 63–73.